

Improving Domain-Invariance in Self-Supervised Learning via Batch Styles Standardization

Marin Scalbert
 Université Paris Saclay
 CentraleSupélec - MICS
 VitaDX, Paris
 marin.scalbert@centralesupelec.fr

Maria Vakalopoulou
 Université Paris Saclay
 CentraleSupélec - MICS
 maria.vakalopoulou@centralesupelec.fr

Florent Couzinié-Devy
 VitaDX, Paris
 f.couzinie-devy@vitadx.com

Abstract

The recent rise of Self-Supervised Learning (SSL) as one of the preferred strategies for learning with limited labeled data, and abundant unlabeled data has led to the widespread use of these models. They are usually pretrained, finetuned, and evaluated on the same data distribution, i.e., within an in-distribution setting. However, they tend to perform poorly in out-of-distribution evaluation scenarios, a challenge that Unsupervised Domain Generalization (UDG) seeks to address.

This paper introduces a novel method to standardize the styles of images in a batch. Batch styles standardization, relying on Fourier-based augmentations, promotes domain invariance in SSL by preventing spurious correlations from leaking into the features. The combination of batch styles standardization with the well-known contrastive-based method SimCLR leads to a novel UDG method named CLaSSy (Contrastive Learning with Standardized Styles). CLaSSy offers serious advantages over prior methods, as it does not rely on domain labels and is scalable to handle a large number of domains. Experimental results on various UDG datasets demonstrate the superior performance of CLaSSy compared to existing UDG methods. Finally, the versatility of the proposed batch styles standardization is demonstrated by extending respectively the contrastive-based and non-contrastive-based SSL methods, SWaV and MSN, while considering different backbone architectures (convolutional-based, transformers-based).

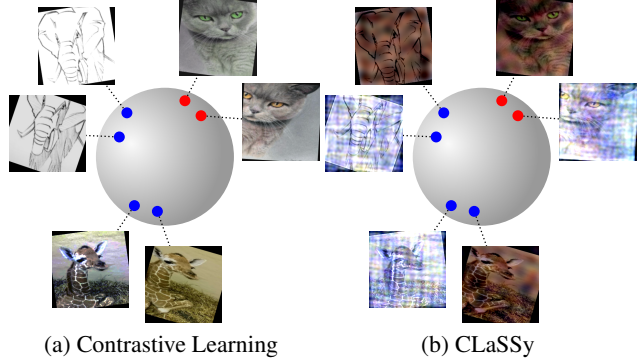


Figure 1. Comparison between regular contrastive learning and CLaSSy. • and ● markers represent positive and negative examples respectively when considering augmented cats as anchors. (a) In Contrastive Learning, examples are augmented independently, which may result in using style information to repel negative from positive examples. (b) CLaSSy standardizes the styles of positive and negative examples using Fourier-based augmentations. Independent augmentations on positive examples promote domain invariance when they are pulled together. Standardizing styles of positive and negative examples prevents style information from leaking into features when repelling negatives from positives.

1. Introduction

Motivations. In recent years, both contrastive and non-contrastive self-supervised learning (SSL) methods, have seen significant growth and success [1, 3, 5, 6, 14, 16]. However, traditional SSL methods make the assumption that training and testing data come from the same distribution, which does not hold true in practice and consequently limits their real-life applications. This so-called domain shift usually leads to poor model generalization on testing

data from unseen domains.

Unsupervised Domain Generalization (UDG), a novel Domain Generalization (DG) setting introduced by [36], aims to tackle this issue by assessing the generalizability of SSL models on data from previously unobserved domains. In this setting, models are first pretrained on unlabeled data and then evaluated through linear probing or finetuning on a DG task. This work focuses only on the all-correlated UDG setting [36] where unlabeled data and the labeled data of the DG task come from the same domains, while testing data come from an unknown target domain.

Current UDG methods, whether they are contrastive-based [15, 36] or not [16], suffer from the same drawbacks: (1) They require domain labels, which in practice may be challenging to obtain or unavailable, and/or (2) have poor scalability to many domains due to architectural constraints such as domain-specific queues or decoders. These limitations highlight the need for more flexible domain-invariant self-supervised methods.

Contributions. This work proposes a novel method for standardizing image styles in a batch, leveraging Fourier-based augmentations [32, 34]. This standardization technique, which transfers the style of a randomly selected image to all images in the batch, promotes domain invariance by preventing style information from leaking into features. It does not entail additional training and has a minimal impact on the computational cost of SSL methods.

The proposed batch style standardization is combined with SimCLR [6], a well-known contrastive-based method, to create a domain-invariant SSL method named CLaSSy (Contrastive Learning with Standardized Styles), illustrated on Fig. 1. Specifically, batch styles standardization in CLaSSy prevents style information leakage when repelling negative examples from positive examples. Somehow, it can also be seen as a means of creating harder negative examples, which has proven to be essential to make the most of contrastive-based methods. Unlike prior approaches, CLaSSy does not require domain labels and can handle any number of domains while showing substantial performance gains on common UDG benchmark datasets.

Finally, the versatility of batch styles standardization is demonstrated by extending its application to both contrastive and non-contrastive methods and different backbones with convolutional or transformers architectures. Experiments using SWaV [3] and MSN [1] methods, coupled with the proposed batch style standardization, highlight the potential of our method. The full code of our method will be released upon acceptance.

2. Related works

Domain Generalization aims to train a model on labeled data from multiple source domains with distinct dis-

tributions to generalize well on unseen target domains. Former DG methods have focused on aligning source feature distributions using diverse techniques [13, 20, 24, 26, 27, 28, 31, 37]. More recently, the trend has shifted towards improving cross-domain generalization through better data augmentation strategies. These strategies can be applied at either the image level [29, 32, 34, 38, 39] or feature representation level [21, 25, 40], and can be non-parametric [32, 40], trained adversarially during the DG task [17, 21, 38, 39], or pretrained beforehand on source domains [29]. Among these methods, Fourier-based augmentations [32, 34] is probably the most simple and promising approach to enhance generalization. We employ this augmentation for its simplicity, efficiency, speed, and particularly for its ability not to require domain labels.

Self-Supervised learning has gained a lot of attraction due to its faculty to efficiently pretrain models on large amounts of unlabeled data. A recent and successful line of SSL research is Contrastive Learning, which focuses on making features of augmented views of the same image (positives) closer in an embedding space while pushing apart features of other examples (negatives). These methods can work either at the instance level [6, 8, 18] or at the cluster level [2, 4], while there have also been attempts to eliminate the use of negative examples due to batch size limitations [1, 5, 9, 14]. In this work, we extend contrastive-based (SimCLR [6], SWaV [3]) and non-contrastive-based (MSN [1]) methods to ease the transfer of pretrained features for solving DG tasks, which corresponds to the UDG problem.

Unsupervised Domain Generalization methods based on Contrastive Learning such as DARLING [36] and BrAD [15] improve domain-invariance in their contrastive losses by ensuring that positive and negative examples belong to the same domain. Restricting comparisons to examples from the same domain prevents the development of spurious correlated features when repelling negative examples from positive ones. To do so, DARLING exploits domain-specific adversarial negative queues while BrAD preserves domain-specific negative queues containing past representations from the momentum encoder. Additionally, BrAD learns image-to-image mappings from the different domains into a shared space and performs contrastive learning between representations of raw and projected images. In [33], Yang *et al.* propose an alternative approach relying on Masked Auto-Encoder [16] (MAE) to solve a cross-domain reconstruction task. More specifically, images styles are augmented using Fourier-based augmentations, then masked, and finally, domain-specific decoders reconstruct and recover the original styles of masked tokens. Masked tokens reconstruction learns semantically coherent features while recovering original styles with domain-specific decoders encourages domain-invariant features.

3. Method

The following sections define the UDG problem, outline the basic Fourier-based augmentations and how they are leveraged for batch styles standardization. Finally CLaSSy, our proposed novel UDG method is introduced.

3.1. Problem formulation

In the all-correlated UDG setting, an unlabeled dataset $D_u = \{(x_i, d_i) \in \mathcal{X} \times \mathcal{D}_S\}_{1 \leq i \leq n_u}$, a labeled dataset $D_l = \{(x_i, y_i, d_i) \in \mathcal{X} \times \mathcal{Y} \times \mathcal{D}_S\}_{1 \leq i \leq n_l}$ and a test dataset $D_t = \{(x_i, y_i, d_i) \in \mathcal{X} \times \mathcal{Y} \times \mathcal{D}_T\}_{1 \leq i \leq n_t}$ are given. The variables x , y and d denote respectively an image, its class label and its domain label while \mathcal{X} , \mathcal{Y} and \mathcal{D} are their respective spaces. In this setting, unlabeled and labeled training data are drawn from the same source domains \mathcal{D}_S and share the same class labels space \mathcal{Y} . Testing data are drawn from an unseen target domain \mathcal{D}_T . The goal of UDG is to pretrain a network on D_u via SSL such that when finetuned on D_l it will generalize well on the data D_t coming from a domain unobserved during the training. Such generalization reflects the ability of the SSL method to learn semantically coherent and domain-invariant features.

3.2. Fourier-based data augmentation

Fourier-based data augmentation is motivated by an established property of the Fourier transform \mathcal{F} : phase components \mathcal{P} of the Fourier transform tend to retain semantic information while amplitude components \mathcal{A} are more related to low-level information such as global colors and textures. Thus, by randomly altering the amplitudes of the images during training, the network can prioritize semantic information over style information.

The Fourier-based data augmentation procedure, illustrated in Fig. 2, consists of the following steps: (1) apply the Fourier transform \mathcal{F} to a source image and a target image, (2) swap low-frequency components of the source image amplitude with that of the target image, and (3) apply the inverse Fourier transform \mathcal{F}^{-1} to return to the image space. The size of the swapped region is controlled by an area ratio hyperparameter $r \in [0, 1]$ representing a ratio between the area of the swapped region and the entire amplitude area. To increase the diversity of the augmented images, rather than fixing the ratio r , we sample it from a uniform distribution $\mathcal{U}(r_{min}, r_{max})$ where r_{min} and r_{max} stand for the minimum and maximum possible ratios.

3.3. Batch styles standardization

We leverage Fourier-based augmentations as a means to project all images in a batch to the same style. To achieve this, the style of a single randomly selected image in the batch is transferred to all other images, creating the impression that they were drawn from the same domain. This

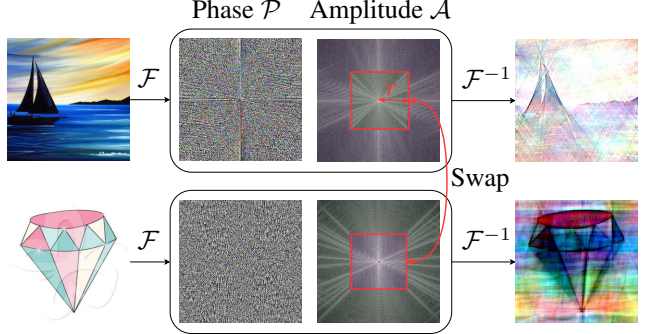


Figure 2. Fourier-based augmentations: Given a pair of images, the Fourier Transform \mathcal{F} is applied on both images. Regions associated with low-frequency components of the amplitude \mathcal{A} , determined by the areas ratio r , are swapped. The inverse \mathcal{F}^{-1} is applied to the altered transforms to project them back to the image space.

batch styles standardization removes the variability associated with styles, thereby preventing the use of style information to solve the SSL task.

More specifically, to perform batch styles standardization, we first randomly select a single image from a batch of N images and then swap the low-frequency amplitudes of the other images with those of the selected image. Each augmented image is then subjected to independent geometrical transformations, while a consistent color augmentation is applied to maintain a common style across all images. This process is repeated V times, generating V augmented views of each image or somehow V augmented batches, each with a unique style/domain. Examples of these augmented batches from two studied datasets are shown in Fig. 3. A Pytorch implementation of batch styles standardization is provided in Appendix A.

3.4. Contrastive Learning with Standardized Styles

CLaSSy, illustrated in Fig. 1, builds upon previous UDG works by incorporating Fourier-based augmentations and ensuring that the compared positive and negative examples belong to the same domain. A notable distinction from prior works is that CLaSSy does not rely on any domain labels. Instead, batch styles standardization is employed to standardize the styles of positive and negative examples making them appear as if they originated from the same domain, without requiring any domain labels.

Specifically, CLaSSy aims to bring representations of images that share the same content but differ in style closer together, while simultaneously repelling representations of different content but sharing the same styles as positive examples. Intuitively, restricting styles among positive and negative examples should prevent style information from affecting features and somehow should create harder neg-

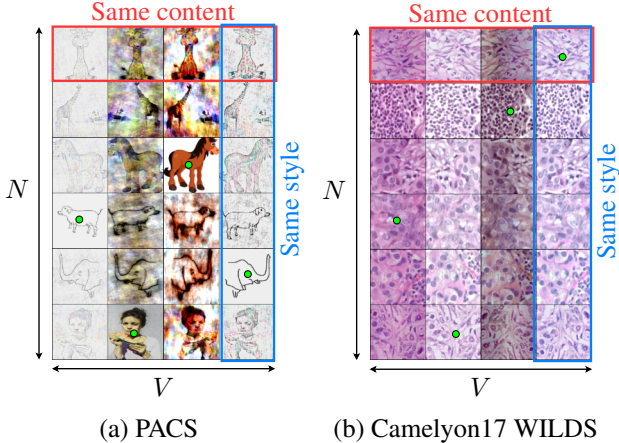


Figure 3. Augmented batches with batch styles standardization on (a) PACS and (b) Camelyon17 WILDS datasets. Given a batch of N images, the amplitudes of each image are swapped with those of a randomly selected image in the batch (indicated by \bullet). This process is repeated V times independently to obtain V augmented views of each image, or somehow V augmented batches, each with a unique style.

ative examples.

To fulfill this goal, once batch styles standardization has been applied, the resulting images are rearranged into a $N \times V$ images grid denoted X , where each row corresponds to a different content c and each column to a different style s , as shown in Fig. 3. Each augmented image x_{cs} is then processed through a backbone, a projection head and normalized with the L^2 -norm to produce its corresponding representation $z_{cs} \in \mathbb{R}^D$. Finally, we minimize the same objective function as in SimCLR [6] combined with a multi-crops strategy [3] including V augmented views. Given an anchor z_{cs} , this corresponds minimizing the following loss per sample:

$$\mathcal{L}_{cs} = -\frac{1}{V-1} \sum_{s' \neq s} \log \left(\frac{e^{z_{cs} \cdot z_{cs'}/T}}{\sum_{(c'', s'') \neq (c, s)} e^{z_{cs} \cdot z_{c''s''}/T}} \right) \quad (1)$$

T stands for a temperature hyperparameter.

4. Results

4.1. Datasets

Extensive experiments were performed on 3 datasets widely used for benchmarking DG / UDG methods, namely **PACS**, **DomainNet** and **Camelyon17 WILDS**.

PACS [23] contains 4 domains (Photo, Art Painting, Cartoon, Sketch) and 7 classes. **DomainNet** [27] contains 6 different domains (clipart, infograph, quickdraw, painting, real and sketch) and covers 345 classes. Following prior UDG

works [15, 33, 36], we consider a subset of DomainNet including 20 classes out of the 345 available classes. **Camelyon17 WILDS** [22] includes 2 classes and 5 domains. The dataset is split into `train`, `val`, and `test` subsets comprising respectively 3, 1, and 1 distinct domains.

4.2. Experimental setup

To evaluate the cross-domain generalization ability of the proposed UDG method, we followed the exact same evaluation protocol described in [36] for the UDG all-correlated setting. Therefore, we first pretrained the backbone network on the source domains in an unsupervised manner using the proposed method. Second, using only a fraction of the source labeled data, we finetuned it or learned a linear classifier on top of the frozen representations (linear probing). Finally, performances were evaluated on data from an unseen target domain. All our networks were trained without Imagenet [11] pretraining, except on DomainNet to allow fair comparisons with prior UDG works (see discussion in 4.3).

Following previous work [15], on **PACS** and **DomainNet**, all the models were evaluated through linear probing except when considering the entire PACS dataset where full-finetuning was performed as in [33, 36]. On **Camelyon17 WILDS**, linear probing was performed for each proportion of labeled data. Additional implementation details about the unsupervised trainings and evaluations are provided in Appendix B.

4.3. UDG performances

PACS. The averaged accuracy over three independent runs, for all possible combinations (sources, target) domains and for different proportions of labeled data are reported on Tab. 1. Our method achieves the highest per-domain averaged accuracy with margins of $+0.63$, $+3.45$, $+0.49$ and $+5.34$ for proportions of labeled data of 1%, 5%, 10% and 100%, respectively. For the 10% proportion, we use linear probing for evaluation, which is similar to BrAD but different from DiMAE. On this proportion, our results show a significant improvement compared to BrAD and still a slightly better performance compared to DiMAE. Regarding accuracy on the different target domains, CLaSSy outperforms its competitors most of the time, except for the target domain photo. This discrepancy may be attributed to the fact that both BrAD and DiMAE benefit from transfer learning on ImageNet while we do not take advantage of any form of transfer learning. On the challenging target domain sketch, due to large visual discrepancies with source domains, our method demonstrates its generalization ability with significant performance gains ranging from $+8.42$ to $+16.33$ for the different proportions of labeled data.

DomainNet. We follow prior UDG works [15, 33, 36] by selecting painting, real and sketch as source domains and

Methods	Label Fraction: 1%					Label Fraction: 5%				
	Target domain					Target domain				
	photo	art	cartoon	sketch	avg.	photo	art	cartoon	sketch	avg.
MoCo V2 [8]	22.97	15.58	23.65	25.27	21.87	37.39	25.57	28.11	31.16	30.56
SimCLR V2 [7]	30.94	17.43	30.16	25.20	25.93	54.67	35.92	35.31	36.84	40.68
BYOL [14]	11.20	14.53	16.21	10.01	12.99	26.55	17.79	21.87	19.65	21.46
AdCo [18]	26.13	17.11	22.96	23.37	22.39	37.65	28.21	28.52	30.35	31.18
MAE [16]	30.72	23.54	20.78	24.52	24.89	32.69	24.61	27.35	30.44	28.77
DARLING [36]	27.78	19.82	27.51	29.54	26.16	44.61	39.25	36.41	36.53	39.20
DiMAE* [33]	<u>48.86</u>	31.73	25.83	32.50	34.73	50.00	41.25	34.40	38.00	40.91
BrAD* [15]	61.81	<u>33.57</u>	<u>43.47</u>	<u>36.37</u>	<u>43.80</u>	65.22	<u>41.35</u>	<u>50.88</u>	<u>50.68</u>	<u>52.03</u>
CLaSSy	45.76	34.85	49.38	47.73	44.43	<u>59.86</u>	43.74	54.97	63.33	55.48
Methods	Label Fraction: 10%					Label Fraction: 100%				
	Target domain					Target domain				
	photo	art	cartoon	sketch	avg.	photo	art	cartoon	sketch	avg.
MoCo V2 [8]	44.19	25.85	35.53	24.97	32.64	59.86	28.58	48.89	34.79	43.03
SimCLR V2 [7]	54.65	37.65	46.00	28.25	41.64	67.45	43.60	54.48	34.73	50.06
BYOL [14]	27.01	25.94	20.98	19.69	23.40	41.42	23.73	30.02	18.78	28.49
AdCo [18]	46.51	30.31	31.45	22.96	32.81	58.59	29.81	50.19	30.45	42.26
MAE [16]	35.89	25.59	33.28	32.39	31.79	36.84	25.24	32.25	34.45	32.20
DARLING [36]	53.37	39.91	46.41	30.17	42.46	68.86	41.53	56.89	37.51	51.20
DiMAE* [33]	77.87	<u>59.77</u>	<u>57.72</u>	39.25	<u>58.65</u>	<u>78.99</u>	63.23	<u>59.44</u>	<u>55.89</u>	<u>64.39</u>
BrAD* [15]	<u>72.17</u>	44.20	50.01	<u>55.66</u>	55.51	X	X	X	X	X
CLaSSy	63.10	<u>48.91</u>	59.27	65.28	59.14	79.77	62.45	64.49	72.22	69.73

* Uses Imagenet pretraining.

Table 1. UDG performances on PACS. Averaged accuracies are reported over three independent runs, for all possible combinations of (sources, target) domains and for different proportions of labeled data. The first and second best performing methods are respectively highlighted in **red** and blue.

the others as target domains. The reversed combination of source and target domains is also considered. For these two combinations, we report on Tab.2, the averaged accuracy per domain and the overall accuracy for different proportions of labeled data (1%, 5% and 10%). The presented results are averaged over three independent runs.

For proportions of 1% and 5%, CLaSSy exhibits superior performance over self-supervised and prior UDG methods on nearly all target domains. It outperforms the previous best UDG method, BrAD, on global metrics (i.e. overall accuracy and per-domain averaged accuracy) with comfortable margins. For the 10% proportion, DiMAE outperforms CLaSSy on the global metrics. However, it is worth noting that in this case, DiMAE is the only method that used full-finetuning for evaluation. When compared to methods employing linear probing for evaluation, CLaSSy still outperforms its competitors.

Camelyon17 WILDS. The averaged accuracy over ten independent runs, for different proportions of labeled data (1%, 5%, 10%, 100%), on the test split of Camelyon17 WILDS are reported on Tab. 3. For fair comparisons, the reimplemented methods DARLING and DiMAE used the same training and evaluation hyperparameters. According to Tab. 3, for any proportion of labeled data, our method

outperforms the other UDG methods (DARLING, DiMAE) with large margins. It even surpasses the Semi-Supervised method FixMatch [30] and the SSL method SWaV [3] that have been trained with additional unlabeled data from the target domain. Compared to the second best-performing UDG method DiMAE, for all the proportions of labeled data, our method yields significant performance gains.

Pretraining in DG/UDG. The usage of pretrained networks in DG is common but we think it is misguided. Often the pretraining dataset includes one or more of the target domains, *e.g.*, *photo* for PACS or *real* for DomainNet when using ImageNet pretraining. When evaluating on these domains, it is not possible to know if the performances are due to real generalization capacity or to simple conservation of the pretrained features. For new methods, it is hard not to follow the common practice because the pretraining unfairly boosts the results of previous works and state-of-the-art performances are often seen as a prerequisite for paper acceptance. We tried to limit the usage of pretraining in our experiments and only used it for the DomainNet dataset. The bias introduced by Imagenet pretraining can be seen in our results and especially for the domains that are close to ImageNet: on PACS (Tab. 1), without pretraining, CLaSSy is consistently the best method for all settings except for

Sources	Paint. \cup Real. \cup Sketch.			Clip. \cup Info. \cup Quick.				
Target	clipart	infograph	quickdraw	painting	real	sketch	Overall	Avg.
Label Fraction 1%								
ERM	6.54	2.96	5.00	6.68	6.97	7.25	5.88	5.90
BYOL [14]	6.21	3.48	4.27	5.00	8.47	4.42	5.61	5.31
MoCo V2 [8]	18.85	10.57	6.32	11.38	14.97	15.28	12.12	12.90
AdCo [18]	16.16	12.26	5.65	11.13	16.53	17.19	12.47	13.15
SimCLR V2 [7]	23.51	15.42	5.29	20.25	17.84	18.85	15.46	16.86
DARLING [36]	18.53	10.62	12.65	14.45	21.68	21.30	16.56	16.54
DiMAE [33]	26.52	15.47	15.47	20.18	30.77	20.03	21.85	21.41
BrAD [15]	47.26	16.89	23.74	20.03	25.08	31.67	25.85	27.45
CLaSSy	61.42	18.93	24.85	28.18	33.84	42.63	32.46	34.98
Label Fraction 5%								
ERM	10.21	7.08	5.34	7.45	6.08	5.00	6.50	6.86
BYOL [14]	9.60	5.09	6.02	9.78	10.73	3.97	7.83	7.53
MoCo V2 [8]	28.13	13.79	9.67	20.80	24.91	21.44	18.99	19.79
AdCo [18]	30.77	18.65	7.75	19.97	24.31	24.19	19.42	20.94
SimCLR V2 [7]	34.03	17.17	10.88	21.35	24.34	27.46	20.89	22.54
DARLING [36]	39.32	19.09	10.50	21.09	30.51	28.49	23.31	24.83
DiMAE [33]	42.31	18.87	15.00	27.02	39.92	26.50	27.85	28.27
BrAD [15]	64.01	25.02	29.64	29.32	34.95	44.09	35.37	37.84
CLaSSy	69.35	19.82	30.28	38.27	41.54	51.75	39.22	41.84
Label Fraction 10%								
ERM	15.10	9.39	7.11	9.90	9.19	5.12	8.94	9.30
BYOL [14]	14.55	8.71	5.95	9.50	10.38	4.45	8.69	8.92
MoCo V2 [8]	32.46	18.54	8.05	25.35	29.91	23.71	21.87	23.00
AdCo [18]	32.25	17.96	11.56	23.35	29.98	27.57	22.79	23.78
SimCLR V2 [7]	37.11	19.87	12.33	24.01	30.17	31.58	24.28	25.84
DARLING [36]	35.15	20.88	15.69	25.90	33.29	30.77	26.09	26.95
DiMAE (finetuned) [33]	70.78	38.06	27.39	50.73	64.89	55.41	49.49	51.21
BrAD [15]	68.27	26.60	34.03	31.08	38.48	48.17	38.74	41.10
CLaSSy	69.81	19.62	30.37	40.43	42.86	53.08	40.06	42.70

Table 2. UDG performances on DomainNet subset. Averaged accuracy is reported over three independent runs, for the specified combinations of (sources, target) domains and for different proportions of labeled data. The first and second best performing methods are respectively highlighted in **red** and **blue**.

Method	Label Fraction			
	1%	5%	10%	100%
DARLING* [36]	70.44	72.00	72.43	72.36
DiMAE* [33]	89.81	89.17	89.77	90.40
FixMatch† [30]	✗	✗	✗	71.00
SWaV‡ [3]	✗	✗	✗	91.40
CLaSSy	92.27	94.75	94.82	95.00

* Our implementation (no available public code).

† As part of Camelyon17 WILDS challenge [22].

‡ Uses unlabeled data from the target domain.

Table 3. UDG performances on Camelyon17 WILDS. Averaged accuracies are reported over ten independent runs and for different proportions of labeled data. The first and second best performing methods are respectively highlighted in **red** and **blue**.

the *photo* domain, where methods using ImageNet pretrain-

ing report better performance. However, on DomainNet (Tab. 2), when using ImageNet pretraining similar to the other methods, CLaSSy is the most performant on the *real* domain (best on 2 out of 3 proportions of labeled data).

4.4. Features visualization

To assess the quality of the learned features and their ability to generalize across domains, we present t-SNE plots of the backbone representations for Camelyon17 WILDS in Fig. 4. DARLING representations tend to be domain-invariant as lots of examples from different domains are superimposed. However, this is also the case for many examples from different classes indicating potentially poor model generalization. In contrast, DiMAE representations appear to be well separated by classes but also by domains, especially for the target domains *hospital_1* and *hospital_2*, indicating a lack of domain-invariance. Finally, better class separability and domain confusion

emerge from our method representations revealing a better domain-invariance and a potentially better cross-domain generalization.

5. Extended experiments

Components ablations. To evaluate the impact of the different components of the method (Fourier-based augmentations, batch styles standardization) on performances, we pretrained the backbone with all possible combinations of components using the same experimental setup and hyperparameters as experiments detailed in 4. The averaged results of this experiment over ten independent runs on the Camelyon17 WILDS dataset for the different proportions of labeled source data are presented in Tab. 4.

		Label Fraction			
Fourier	BSS	1%	5%	10%	100%
✗	✗	63.54	63.58	63.50	65.06
✗	✓	66.81	68.19	68.45	68.53
✓	✗	91.07	91.95	91.99	92.15
✓	✓	92.27	94.75	94.82	95.00

Table 4. Ablation studies on the different components of the method (Fourier-based augmentations, Styles standardization). Averaged accuracy on Camelyon17 WILDS over ten independent runs and for different proportions of labeled source data are reported. (BSS : Batch Styles Standardization)

Our experiments show that the absence of Fourier-based augmentations and styles standardization, resulting in a regular SimCLR approach, leads to relatively low accuracy on the target domain for all proportions of labeled data. Conversely, applying the same color augmentations to both positives and negatives, thereby standardizing only the styles, results in improved generalization performance, with an average accuracy gain of 3 for various proportions of labeled data. This indicates that even reducing the styles variation between positives and negatives helps to learn domain-invariant features.

Fourier-based augmentations alone lead to drastic performance improvements compared to the regular SimCLR. Combining Fourier-based augmentations with styles standardization leads to even greater performance improvements than the regular SimCLR. It is worth noting that adding the styles standardization to Fourier-based augmentations results in substantial performance gains (+1.2, +2.8, +2.83, and +2.85) for the proportions of labeled data 1%, 5%, 10%, and 100%, respectively. These observations support the effectiveness of Fourier-based augmentations and the proposed styles standardization in enhancing domain-invariance in contrastive learning.

Behavior under smaller batch sizes. The sensitivity of contrastive learning-based methods to batch size and the

need for hard negative examples are major challenges. Various methods have attempted to tackle these challenges by using a larger set of negatives [8], exploiting harder negatives [18, 19], or eliminating the need for negatives [9, 14]. To investigate the effect of batch styles standardization on reducing sensitivity to batch size and/or creating harder negatives, we trained our method with or without batch styles standardization for different batch sizes on the Camelyon17 WILDS dataset. Apart from the batch size, the learning rate linearly scaled with respect to batch size, and using a LARS optimizer [35], hyperparameters remained unchanged. The accuracy for each batch size and the method with or without batch styles standardization are reported in Fig. 5.

Overall, using batch styles standardization leads to improved performance for any batch size. As batch size increases, performances increase until a plateau is reached. However, when batch styles standardization is used (indicated by the orange curve), the plateau is reached at smaller batch sizes. Specifically, with batch styles standardization, performance seems to cap beyond a batch size of 64, while without batch styles standardization, performance continues to increase until a batch size of 128. This finding supports the assumption that batch styles standardization helps reduce the sensitivity of contrastive learning to batch size by generating more challenging negative examples.

6. Batch styles standardization for other SSL methods

In this section, to demonstrate the versatility of the proposed batch styles standardization technique and its effectiveness in reinforcing domain-invariance in SSL methods, the respective contrastive and non-contrastive based methods SWaV (SWapping Assignments between multiple Views of the same image) [3] and MSN [1] (Masked Siamese Networks) are extended.

Preamble. SWaV and MSN assign respectively global views or non-masked views of images to prototypes and try to predict these assignments using local or masked views of the same images. To uniformly assign the representations of global or non-masked views to the prototypes, these methods use the online Sinkhorn-Klopp algorithm [10]. We encourage the readers to refer to original publications or Appendix C for further technical details. We hypothesize that the presence of several domains/styles during the online assignments of global or non-masked views may lead to problems. Specifically, if a batch of global or non-masked views includes images from multiple domains/styles, the assignments may correlate with these domains/styles, resulting in a matching between prototypes and styles.

Extensions. To overcome this problem, we propose to enforce a single style for global views or non-masked views using our proposed batch styles standardization technique. Intuitively, restraining the styles to a single style should pre-

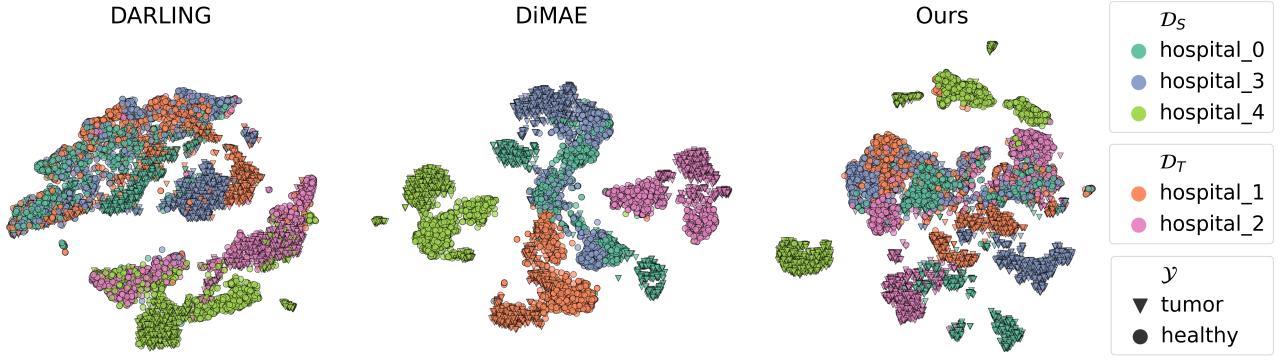


Figure 4. t-SNE plots of the backbone representations for different UDG methods on Camelyon17 WILDS. On the target domains, our method shows better domain confusion while keeping better class separability. Display on pdf with larger zoom for better visualization.

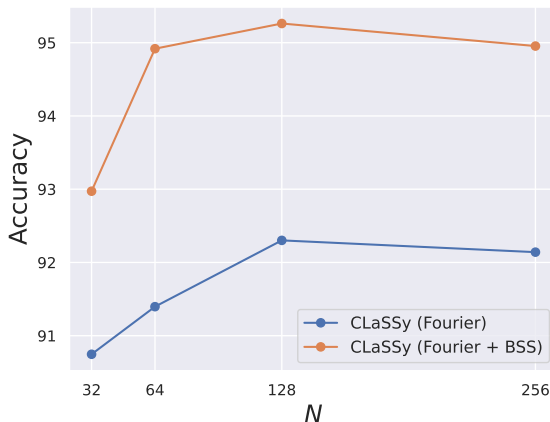


Figure 5. UDG performances of CLaSSy with or without batch styles standardization (BSS) with respect to different batch sizes on the Camelyon17 WILDS dataset.

vent domain/style information from leaking into the resulting assignments, consequently making assignments more semantically relevant. All local and masked views are augmented independently.

To verify the previous hypothesis and evaluate the proposed solution, SWaV and MSN were trained with or without the extension based on batch styles standardization and evaluated using the same experimental setup. We report on Tab. 5, for the Camelyon17 WILDS dataset and different proportions of labeled data, the averaged accuracy of SWaV and MSN without the proposed extension along with the absolute accuracy gains resulting from the extension. For further implementation details and additional hyperparameters of SWaV and MSN, readers may refer to the Appendix C.

The initial findings reveal that the methods combined only with Fourier-based augmentations yields already relatively good results. Incorporating batch styles

Method	Backbone	Components		Label Fraction			
		Fourier	BSS.	1%	5%	10%	100%
CLaSSy	ResNet50	✓	✗	91.07	91.95	91.99	92.15
		✓	✓	↑+1.20	↑+2.80	↑+2.83	↑+2.85
SWaV [3]	ResNet50	✓	✗	91.03	91.94	91.96	92.26
		✓	✓	↑+2.39	↑+2.05	↑+2.11	↑+1.82
MSN [1]	ViT-S/8 [12]	✓	✗	87.07	87.33	87.55	88.22
		✓	✓	↑+3.86	↑+4.49	↑+4.28	↑+3.76

Table 5. Absolute accuracy gains due to batch styles standardization (BSS) on Camelyon17 WILDS for CLaSSy, SWaV and MSN.

standardization to SWaV and MSN results in a significant boost of performances. It is important to notice that batch styles standardization improves contrastive/non-contrastive-based methods under different backbone architectures (convolutional-based and transformer-based). All these observations confirm that Fourier-based augmentation and batch styles standardization can be very efficient in reinforcing domain invariance for self-supervised methods.

7. Conclusion

This paper introduces a new approach for the UDG problem where image styles in a batch are standardized using Fourier-based augmentations. Building on this technique, we propose a novel contrastive-based UDG method named CLaSSy. Unlike other UDG methods, CLaSSy does not require domain labels and can handle any number of domains while achieving superior results on several benchmark datasets. Furthermore, we demonstrate that our batch styles standardization technique can be easily integrated into other SSL methods, including both contrastive and non-contrastive approaches, and can accommodate various backbone architectures, including convolutional-based and transformers-based architectures. Overall, our work provides new avenues to enhance domain invariance in SSL and improve the performance of existing methods.

References

[1] Mahmoud Assran, Mathilde Caron, Ishan Misra, Piotr Bojanowski, Florian Bordes, Pascal Vincent, Armand Joulin, Mike Rabbat, and Nicolas Ballas. Masked siamese networks for label-efficient learning. In *European Conference on Computer Vision*, pages 456–473. Springer, 2022. [1](#), [2](#), [7](#), [8](#)

[2] Mathilde Caron, Piotr Bojanowski, Armand Joulin, and Matthijs Douze. Deep clustering for unsupervised learning of visual features. In *Proceedings of the European conference on computer vision (ECCV)*, pages 132–149, 2018. [2](#)

[3] Mathilde Caron, Ishan Misra, Julien Mairal, Priya Goyal, Piotr Bojanowski, and Armand Joulin. Unsupervised learning of visual features by contrasting cluster assignments. *Advances in Neural Information Processing Systems*, 33:9912–9924, 2020. [1](#), [2](#), [4](#), [5](#), [6](#), [7](#), [8](#)

[4] Mathilde Caron, Ishan Misra, Julien Mairal, Priya Goyal, Piotr Bojanowski, and Armand Joulin. Unsupervised learning of visual features by contrasting cluster assignments. *Advances in Neural Information Processing Systems*, 33:9912–9924, 2020. [2](#)

[5] Mathilde Caron, Hugo Touvron, Ishan Misra, Hervé Jégou, Julien Mairal, Piotr Bojanowski, and Armand Joulin. Emerging properties in self-supervised vision transformers. In *Proceedings of the IEEE/CVF International Conference on Computer Vision*, pages 9650–9660, 2021. [1](#), [2](#)

[6] Ting Chen, Simon Kornblith, Mohammad Norouzi, and Geoffrey Hinton. A simple framework for contrastive learning of visual representations. In *International conference on machine learning*, pages 1597–1607. PMLR, 2020. [1](#), [2](#), [4](#)

[7] Ting Chen, Simon Kornblith, Kevin Swersky, Mohammad Norouzi, and Geoffrey E Hinton. Big self-supervised models are strong semi-supervised learners. *Advances in neural information processing systems*, 33:22243–22255, 2020. [5](#), [6](#)

[8] Xinlei Chen, Haoqi Fan, Ross Girshick, and Kaiming He. Improved baselines with momentum contrastive learning. *arXiv preprint arXiv:2003.04297*, 2020. [2](#), [5](#), [6](#), [7](#)

[9] Xinlei Chen and Kaiming He. Exploring simple siamese representation learning. In *Proceedings of the IEEE/CVF conference on computer vision and pattern recognition*, pages 15750–15758, 2021. [2](#), [7](#)

[10] Marco Cuturi. Sinkhorn distances: Lightspeed computation of optimal transport. *Advances in neural information processing systems*, 26, 2013. [7](#)

[11] Jia Deng, Wei Dong, Richard Socher, Li-Jia Li, Kai Li, and Li Fei-Fei. Imagenet: A large-scale hierarchical image database. In *2009 IEEE conference on computer vision and pattern recognition*, pages 248–255. Ieee, 2009. [4](#)

[12] Alexey Dosovitskiy, Lucas Beyer, Alexander Kolesnikov, Dirk Weissenborn, Xiaohua Zhai, Thomas Unterthiner, Mostafa Dehghani, Matthias Minderer, Georg Heigold, Sylvain Gelly, et al. An image is worth 16x16 words: Transformers for image recognition at scale. *arXiv preprint arXiv:2010.11929*, 2020. [8](#)

[13] Yaroslav Ganin, Evgeniya Ustinova, Hana Ajakan, Pascal Germain, Hugo Larochelle, François Laviolette, Mario Marchand, and Victor Lempitsky. Domain-adversarial training of neural networks. *The journal of machine learning research*, 17(1):2096–2030, 2016. [2](#)

[14] Jean-Bastien Grill, Florian Strub, Florent Altché, Corentin Tallec, Pierre Richemond, Elena Buchatskaya, Carl Doersch, Bernardo Avila Pires, Zhaohan Guo, Mohammad Gheshlaghi Azar, et al. Bootstrap your own latent-a new approach to self-supervised learning. *Advances in neural information processing systems*, 33:21271–21284, 2020. [1](#), [2](#), [5](#), [6](#), [7](#)

[15] Sivan Harary, Eli Schwartz, Assaf Arbelle, Peter Staar, Shady Abu-Hussein, Elad Amrani, Roei Herzig, Amit Alfassy, Raja Giryes, Hilde Kuehne, et al. Unsupervised domain generalization by learning a bridge across domains. In *Proceedings of the IEEE/CVF Conference on Computer Vision and Pattern Recognition*, pages 5280–5290, 2022. [2](#), [4](#), [5](#), [6](#)

[16] Kaiming He, Xinlei Chen, Saining Xie, Yanghao Li, Piotr Dollár, and Ross Girshick. Masked autoencoders are scalable vision learners. In *Proceedings of the IEEE/CVF Conference on Computer Vision and Pattern Recognition*, pages 16000–16009, 2022. [1](#), [2](#), [5](#)

[17] Judy Hoffman, Eric Tzeng, Taesung Park, Jun-Yan Zhu, Phillip Isola, Kate Saenko, Alexei Efros, and Trevor Darrell. Cycada: Cycle-consistent adversarial domain adaptation. In *International conference on machine learning*, pages 1989–1998. Pmlr, 2018. [2](#)

[18] Qianjiang Hu, Xiao Wang, Wei Hu, and Guo-Jun Qi. Adco: Adversarial contrast for efficient learning of unsupervised representations from self-trained negative adversaries. In *Proceedings of the IEEE/CVF Conference on Computer Vision and Pattern Recognition*, pages 1074–1083, 2021. [2](#), [5](#), [6](#), [7](#)

[19] Yannis Kalantidis, Mert Bulent Sarıyıldız, Noe Pion, Philippe Weinzaepfel, and Diane Larlus. Hard negative mixing for contrastive learning. *Advances in Neural Information Processing Systems*, 33:21798–21809, 2020. [7](#)

[20] Guoliang Kang, Lu Jiang, Yi Yang, and Alexander G Hauptmann. Contrastive adaptation network for unsupervised domain adaptation. In *Proceedings of the IEEE/CVF conference on computer vision and pattern recognition*, pages 4893–4902, 2019. [2](#)

[21] Juwon Kang, Sohyun Lee, Namyup Kim, and Suha Kwak. Style neophile: Constantly seeking novel styles for domain generalization. In *Proceedings of the IEEE/CVF Conference on Computer Vision and Pattern Recognition*, pages 7130–7140, 2022. [2](#)

[22] Pang Wei Koh, Shiori Sagawa, Henrik Marklund, Sang Michael Xie, Marvin Zhang, Akshay Balsubramani, Weihua Hu, Michihiro Yasunaga, Richard Lanas Phillips, Irena Gao, et al. Wilds: A benchmark of in-the-wild distribution shifts. In *International Conference on Machine Learning*, pages 5637–5664. PMLR, 2021. [4](#), [6](#)

[23] Da Li, Yongxin Yang, Yi-Zhe Song, and Timothy M Hospedales. Deeper, broader and artier domain generalization. In *Proceedings of the IEEE international conference on computer vision*, pages 5542–5550, 2017. [4](#)

[24] Haoliang Li, Sinno Jialin Pan, Shiqi Wang, and Alex C Kot. Domain generalization with adversarial feature learning. In

Proceedings of the IEEE conference on computer vision and pattern recognition, pages 5400–5409, 2018. 2

[25] Pan Li, Da Li, Wei Li, Shaogang Gong, Yanwei Fu, and Timothy M Hospedales. A simple feature augmentation for domain generalization. In *Proceedings of the IEEE/CVF International Conference on Computer Vision*, pages 8886–8895, 2021. 2

[26] Ya Li, Xinmei Tian, Mingming Gong, Yajing Liu, Tongliang Liu, Kun Zhang, and Dacheng Tao. Deep domain generalization via conditional invariant adversarial networks. In *Proceedings of the European Conference on Computer Vision (ECCV)*, pages 624–639, 2018. 2

[27] Xingchao Peng, Qinxun Bai, Xide Xia, Zijun Huang, Kate Saenko, and Bo Wang. Moment matching for multi-source domain adaptation. In *Proceedings of the IEEE/CVF international conference on computer vision*, pages 1406–1415, 2019. 2, 4

[28] Marin Scalbert, Maria Vakalopoulou, and Florent Couzinié-Devy. Multi-source domain adaptation via supervised contrastive learning and confident consistency regularization. *arXiv preprint arXiv:2106.16093*, 2021. 2

[29] Marin Scalbert, Maria Vakalopoulou, and Florent Couzinié-Devy. Test-time image-to-image translation ensembling improves out-of-distribution generalization in histopathology. In *International Conference on Medical Image Computing and Computer-Assisted Intervention*, pages 120–129. Springer, 2022. 2

[30] Kihyuk Sohn, David Berthelot, Nicholas Carlini, Zizhao Zhang, Han Zhang, Colin A Raffel, Ekin Dogus Cubuk, Alexey Kurakin, and Chun-Liang Li. Fixmatch: Simplifying semi-supervised learning with consistency and confidence. *Advances in neural information processing systems*, 33:596–608, 2020. 5, 6

[31] Eric Tzeng, Judy Hoffman, Ning Zhang, Kate Saenko, and Trevor Darrell. Deep domain confusion: Maximizing for domain invariance. *arXiv preprint arXiv:1412.3474*, 2014. 2

[32] Qinwei Xu, Ruipeng Zhang, Ya Zhang, Yanfeng Wang, and Qi Tian. A fourier-based framework for domain generalization. In *Proceedings of the IEEE/CVF Conference on Computer Vision and Pattern Recognition*, pages 14383–14392, 2021. 2

[33] Haiyang Yang, Shixiang Tang, Meilin Chen, Yizhou Wang, Feng Zhu, Lei Bai, Rui Zhao, and Wanli Ouyang. Domain invariant masked autoencoders for self-supervised learning from multi-domains. In *European Conference on Computer Vision*, pages 151–168. Springer, 2022. 2, 4, 5, 6

[34] Yanchao Yang and Stefano Soatto. Fda: Fourier domain adaptation for semantic segmentation. In *Proceedings of the IEEE/CVF Conference on Computer Vision and Pattern Recognition*, pages 4085–4095, 2020. 2

[35] Yang You, Igor Gitman, and Boris Ginsburg. Large batch training of convolutional networks. *arXiv preprint arXiv:1708.03888*, 2017. 7

[36] Xingxuan Zhang, Linjun Zhou, Renzhe Xu, Peng Cui, Zheyuan Shen, and Haoxin Liu. Towards unsupervised domain generalization. In *Proceedings of the IEEE/CVF Conference on Computer Vision and Pattern Recognition*, pages 4910–4920, 2022. 2, 4, 5, 6

[37] Shanshan Zhao, Mingming Gong, Tongliang Liu, Huan Fu, and Dacheng Tao. Domain generalization via entropy regularization. *Advances in Neural Information Processing Systems*, 33:16096–16107, 2020. 2

[38] Kaiyang Zhou, Yongxin Yang, Timothy Hospedales, and Tao Xiang. Deep domain-adversarial image generation for domain generalisation. In *Proceedings of the AAAI Conference on Artificial Intelligence*, volume 34, pages 13025–13032, 2020. 2

[39] Kaiyang Zhou, Yongxin Yang, Timothy Hospedales, and Tao Xiang. Learning to generate novel domains for domain generalization. In *European conference on computer vision*, pages 561–578. Springer, 2020. 2

[40] Kaiyang Zhou, Yongxin Yang, Yu Qiao, and Tao Xiang. Domain generalization with mixstyle. *arXiv preprint arXiv:2104.02008*, 2021. 2

A. Pytorch implementation of Batch Styles Standardization

On Listing 1, a Pytorch implementation of the batch styles standardization is provided.

B. Implementation details

B.1. Unsupervised training

On **PACS** and **DomainNet**, we train ResNet18 [8] for 60K steps with respective batch sizes of $N = 256$ and $N = 512$, using $V = 2 \times 224^2 + 6 \times 128^2$ crops. Our data augmentation includes geometrical augmentations such as random cropping, horizontal flips, small rotations, and cutout[5], batch styles standardization with $(r_{min}, r_{max}) = (0.02, 1)$, and color augmentations based on RandAugment [2].

On **Camelyon17 WILDS**, we train ResNet50 [8] for 150K steps with a batch size of $N = 256$ and $V = 8 \times 128^2$ crops. We apply geometric augmentations such as random cropping, flips, rotations, and cutout, as well as batch styles standardization with $(r_{min}, r_{max}) = (0.02, 0.10)$, and color augmentations using color jitter.

For all datasets, the projection head hidden representations dimension is set to 2048 and the final representation dimension to $D = 128$ as in [1]. We use a temperature of $T = 0.5$, Adam optimization method [10] with an initial learning rate of 10^{-4} and a learning rate with cosine decay schedule. All our networks are trained without Imagenet [4] pretraining, except on DomainNet to allow fair comparisons with prior UDG works. All trainings were performed on a single NVIDIA Tesla V100 GPU with 32 GB of GRAM.

B.2. Evaluation

For all datasets (**PACS**, **DomainNet**, and **Camelyon17 WILDS**), we use the Adam optimization method [10] with an initial learning rate of 10^{-4} , a learning rate scheduler with cosine decay, and weight decay of 10^{-4} . The networks are trained respectively for 5K, 1K, and 15K steps with batch sizes of 128, 64, and 64. When performing linear probing, we follow the same normalization scheme as [7] by adding a batch normalization layer [9] without affine parameters before the linear classifier.

C. Technical details of extended SSL methods

C.1. SWaV

In SWaV, the same image x is transformed into two augmented views, denoted as $x^{(s)}$ and $x^{(t)}$. These views are processed by the backbone and the projection head. The resulting representations are then projected onto a unit sphere to obtain their final form denoted as $z^{(s)}$ and $z^{(t)}$. Batches of these normalized representations, $Z^{(s)}$ and $Z^{(t)}$, are used to compute the codes $Q^{(s)}$ and $Q^{(t)}$, which correspond to

soft assignments of the representations over K prototypes denoted $\mathbf{C} \in \mathbb{R}^{K \times D}$. The codes are computed online using Sinkhorn-Klopp [3] so that all examples in a batch are evenly assigned among the prototypes preventing the same assignment for all representations in the batch.

The core idea behind SWaV is that if two features $z^{(s)}$ and $z^{(t)}$ represent the same information (i.e. they derive from the same image), it should be possible to predict $q^{(t)}$ from $z^{(s)}$ and $q^{(s)}$ from $z^{(t)}$. This is the essence of the "swapping" concept in SWaV. Therefore, SWaV minimizes the following loss per sample:

$$\ell = H(q_n^{(s)}, p_n^{(t)}) + H(q_n^{(t)}, p_n^{(s)}) \quad (1)$$

$H(p, q)$ stands for the cross-entropy between the approximated probability distribution q and the true probability distribution p while $p_n^{(s)}$ and $p_n^{(t)}$ correspond respectively to assignment probability distributions of $z_n^{(s)}$ or $z_n^{(t)}$ to the prototypes and are defined by:

$$p_n^{(s)} = \text{softmax} \left(\frac{z_n^{(s)} \cdot \mathbf{C}^T}{\tau} \right) \quad (2)$$

$$p_n^{(t)} = \text{softmax} \left(\frac{z_n^{(t)} \cdot \mathbf{C}^T}{\tau} \right) \quad (3)$$

$$(4)$$

τ stands for a temperature hyperparameter and is only used during the computations of $p_n^{(s)}$ and $p_n^{(t)}$.

In practice, to improve the learned representations, a multi-crops strategy including 2 global views and V local views of each image is used. In this setting, the 2 global views are used to compute the codes and the $V + 2$ views representations are used to compute the assignment probabilities. This results in minimizing the following loss per sample:

$$\ell = \frac{1}{2(V-1)} \sum_{i=1}^2 \sum_{v=1}^{V+2} \mathbb{1}_{i \neq v} H(q_n^{(i)}, p_n^{(v)}) \quad (5)$$

C.2. MSN

In MSN, the same image is transformed into several augmented views. Some augmented views are masked (anchors) and others are unmasked (targets). Anchor and target views are respectively processed by an online encoder and a momentum encoder and are all assigned to K prototypes. To ensure, that anchor views are assigned uniformly among prototypes, the entropy of the averaged anchors assignment is maximized while, similarly to SWaV, target views assignments are computed using Sinkhorn-Klopp algorithm [3]. Finally, MSN tries to predict the target views (unmasked) assignments from anchor views (masked) assignments.

```

class BatchStylesStandardization():

    """Implements Batch Styles Standardization. Given a
    batch of  $N$  images, we first randomly select a
    single image from the batch and then swap the
    low-frequency amplitudes of the other images
    with those of the selected image.

    Attributes:
        ratios (tuple): $(r_{min}, r_{max})$ specifying
            the minimum and maximum possible sampled
            area ratio.

    """

    def __init__(self, ratios):
        self.ratios = ratios

    def swap_low_freq(self, src_amp, tgt_amp, ratio):
        """Swap source images amplitudes with target
        images amplitudes. Altered source
        amplitudes are returned.

        Args:
            src_amp (torch.Tensor): Source images
                amplitudes
            tgt_amp (torch.Tensor): Target images
                amplitudes
            ratio (float): Ratio to determine
                swapped area size

        Returns:
            torch.Tensor: Altered source images
                amplitudes
        """

        # Compute center coordinates of amplitudes
        h, w = src_amp.shape[-2:]
        hc, wc = int(h//2), int(w//2)

        # Compute half length of the squared
        # region to be swapped: 1
        l = min([int(ratio*h/2), int(ratio*w/2)])

        # Swap source and target amplitudes
        swapped_tgt_amp = tgt_amp[
            ..., hc-l:hc+l, wc-l:wc+l]
        src_amp[
            ..., hc-l:hc+l, wc-l:wc+l] = swapped_tgt_amp
        return src_amp

    def __call__(self, imgs, n_views):
        """Apply batch styles standardization  $n\_views$  times
        on a batch of images.

        Args:
            imgs (torch.Tensor): Batch of images (N, 3, H, W)
            n_views (int): Number of augmented views

        Returns:
            torch.Tensor: Batch with standardized styles
            (N, n_views, 3, H, W)
        """

        # Apply FFT on source images
        fft = torch.fft.fftn(
            imgs, dim=(-2, -1))
        # Shift low-frequency components to the center
        fft = torch.fft.fftshift(
            fft, dim=(-2, -1))
        # Retrieve amplitude and phase
        amp, phase = fft.abs(), fft.angle()

        # Sample  $n\_views$  images that will be used as
        # ref styles
        bs = imgs.size(0)
        sampled_ind = torch.randperm(bs)[:, :n_views]

        # Swap src amplitudes with those of the  $n\_views$ 
        # sampled images
        src_amp = amp.unsqueeze(1).repeat(
            [1, n_views, 1, 1, 1])
        tgt_amp = amp[sampled_ind].unsqueeze(0).expand(
            bs, -1, -1, -1, -1)
        sampled_ratio = random.uniform(*self.ratios)
        amp = self.swap_low_freq(
            src_amp, tgt_amp, sampled_ratio)

        phase = phase.unsqueeze(1)
        # Reconstruct FFT from amp and phase
        fft = torch.polar(amp, phase)
        # Shift back low-frequency to their
        # original positions
        fft = torch.fft.ifftshift(fft, dim=(-2, -1))
        # Invert FFT
        imgs = torch.fft.ifftn(
            fft, dim=(-2, -1)).real.clamp(0, 1)
        return imgs

```

Listing 1: Pytorch batch styles standardization implementation

More formally, given a batch of N images denoted $\{x_i\}_{1 \leq i \leq N}$, each image x_i is augmented to obtain M anchor views $\{x_{i,1}, \dots, x_{i,M}\}$ and a target view x_i^+ . Anchor views are masked and processed by an online encoder while target views are processed via a momentum encoder whose weights are updated through exponential moving average.

Let $\mathbf{C} \in \mathbb{R}^{K \times D}$ denote the K prototypes and $\{z_{i,1}, \dots, z_{i,M}\}, z_i^+$, the respective representations of anchor and target views, anchors and target views assignments to prototypes can be computed as the following:

$$\begin{cases} p_{i,m} = \text{softmax} \left(\frac{z_{i,m} \cdot \mathbf{C}^T}{\tau} \right) \\ p_i^+ = \text{softmax} \left(\frac{z_i^+ \cdot \mathbf{C}^T}{\tau^+} \right) \end{cases} \quad (6)$$

where τ and τ^+ are standing for temperature hyperparameter. Usually, they are chosen such that $\tau > \tau^+$ to encourage sharper target assignments, which implicitly guides the model to produce confident anchor assignments. Finally, MSN minimizes the following objective function \mathcal{L} :

$$\begin{cases} \mathcal{L} = \frac{1}{NM} \sum_{i=1}^N \sum_{m=1}^M H(p_i^+, p_{i,m}) - \lambda H(\bar{p}) \\ \bar{p} = \frac{1}{NM} \sum_{i=1}^N \sum_{m=1}^M p_{i,m} \end{cases} \quad (7)$$

$H(\bar{p})$ denotes the entropy of the averaged anchors assignment

C.3. Implementation details for extended methods

The hyperparameters used during the extensions of SWaV and MSN are respectively provided in Tab. 1 and Tab. 2.

backbone	ResNet-50 [8]
image initial shape	128 ²
cropping strategy	random crop resizing
global views	2 × 128 ²
local views	6 × 128 ²
(r_{min}, r_{max})	(0.02, 0.1)
K	256
D	128
τ	0.1
N	256
steps	150K
optimizer	LARS [11]
learning rate	0.2
learning rate schedule	cosine decay
weight decay	10 ⁻⁶

Table 1. Hyperparameters used for SWaV extension based on Batch Styles Standardization

backbone	ViT-S/8 [6]
image initial shape	128 ²
cropping strategy	random cropping
target views	2 × 96 ²
anchor views	10 × 64 ²
(r_{min}, r_{max})	(0.02, 0.1)
patch masking ratio	0.3
K	128
D	384
τ	0.1
τ^+	0.025
N	256
steps	150K
Optimizer	LARS [11]
learning rate	0.2
learning rate schedule	cosine decay
weight decay	10 ⁻⁶
EMA momentum	0.995

Table 2. Hyperparameters used for MSN extension based on Batch Styles Standardization

D. Acknowledgments

Experiments have been conducted using HPC resources from the **”Mésocentre”** computing center of Centrale-Supélec and École Normale Supérieure Paris-Saclay, and **”Jean-Zay”** cluster of GENCI (Grand Équipement National du Calcul Intensif).

References

- [1] Ting Chen, Simon Kornblith, Mohammad Norouzi, and Geoffrey Hinton. A simple framework for contrastive learning of visual representations. In *International conference on machine learning*, pages 1597–1607. PMLR, 2020. 1
- [2] Ekin D Cubuk, Barret Zoph, Jonathon Shlens, and Quoc V Le. Randaugment: Practical automated data augmentation with a reduced search space. In *Proceedings of the IEEE/CVF conference on computer vision and pattern recognition workshops*, pages 702–703, 2020. 1
- [3] Marco Cuturi. Sinkhorn distances: Lightspeed computation of optimal transport. *Advances in neural information processing systems*, 26, 2013. 1
- [4] Jia Deng, Wei Dong, Richard Socher, Li-Jia Li, Kai Li, and Li Fei-Fei. Imagenet: A large-scale hierarchical image database. In *2009 IEEE conference on computer vision and pattern recognition*, pages 248–255. Ieee, 2009. 1
- [5] Terrance DeVries and Graham W Taylor. Improved regularization of convolutional neural networks with cutout. *arXiv preprint arXiv:1708.04552*, 2017. 1
- [6] Alexey Dosovitskiy, Lucas Beyer, Alexander Kolesnikov, Dirk Weissenborn, Xiaohua Zhai, Thomas Unterthiner, Mostafa Dehghani, Matthias Minderer, Georg Heigold, Sylvain Gelly, et al. An image is worth 16x16 words: Transformers for image recognition at scale. *arXiv preprint arXiv:2010.11929*, 2020. 3
- [7] Kaiming He, Xinlei Chen, Saining Xie, Yanghao Li, Piotr Dollár, and Ross Girshick. Masked autoencoders are scalable vision learners. In *Proceedings of the IEEE/CVF Conference on Computer Vision and Pattern Recognition*, pages 16000–16009, 2022. 1
- [8] Kaiming He, Xiangyu Zhang, Shaoqing Ren, and Jian Sun. Deep residual learning for image recognition. In *Proceedings of the IEEE conference on computer vision and pattern recognition*, pages 770–778, 2016. 1, 3
- [9] Sergey Ioffe and Christian Szegedy. Batch normalization: Accelerating deep network training by reducing internal covariate shift. In *International conference on machine learning*, pages 448–456. pmlr, 2015. 1
- [10] Diederik P Kingma and Jimmy Ba. Adam: A method for stochastic optimization. *arXiv preprint arXiv:1412.6980*, 2014. 1
- [11] Yang You, Igor Gitman, and Boris Ginsburg. Large batch training of convolutional networks. *arXiv preprint arXiv:1708.03888*, 2017. 3